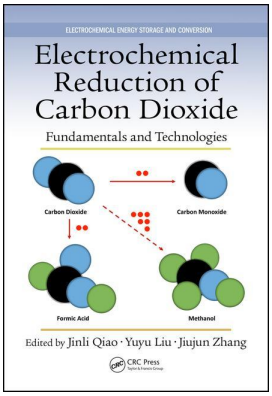

Electrochemical Reduction of Carbon Dioxide Fundamentals and Technologies

Jinli Qiao, Yuyu Liu, Jiujun Zhang

Photoelectrochemical Reduction of CO Electroreduction

Publication details
https://test.routledgehandbooks.com/doi/10.1201/b20177-10
Jinli Qiao, Yuyu Liu, Jiujun Zhang
Published online on: 14 Jun 2016

9 Photoelectrochemical Reduction of CO_2 Electroreduction

Xiaomin Wang

CONTENTS

9.1 INTRODUCTION TO PHOTOELECTROCHEMICAL REDUCTION OF CO_2

9.1.1 General Introduction

Today, humans are facing three serious problems related to energy resources: shortage of energy, shortage of carbon resources, and the global warming problem. In the biosphere, photosynthesis has been employed for both conversion of CO_2 to organics and conversion of solar energy to chemical energy. Oil, coal, and natural gas, which were produced by photosynthesis in ancient times, are finally burnt as

both major energy resources and chemical resources. For solving all three of these problems at once, one of the best solutions is the development of practical systems for converting CO_2 to useful chemicals using solar light. Research of photochemical and photoelectrochemical (PEC) reduction of CO_2 grew rapidly in the past few decades. This was a direct result by growing research from scientists who studied the increasing amount of CO_2 in the atmosphere and the global growing demand of fossil fuel.

The catalytic conversion of CO_2 to liquid fuels is a critical goal that would positively impact the global carbon balance by recycling CO_2 into usable fuels. As an extremely stable molecule generally produced by fossil fuel combustion and respiration, returning CO_2 to a useful state by activation/reduction is a scientifically challenging problem, requiring appropriate catalysts and energy input. This poses several fundamental challenges in chemical catalysis, electrochemistry, photochemistry, and semiconductor physics and engineering.

Photocatalysts for CO_2 reduction are one of the most important aspects of artificial photosynthesis. Consideration of the thermodynamics of CO_2 reduction gives an important strategy for constructing these photocatalysts [1,2]. Equations 9.1 through 9.6 indicate that the one-electron reduction of CO_2 (at pH 7 in an aqueous solution vs. normal hydrogen electrode [NHE]) is highly endothermic and that the product (CO_2) is too reactive to handle with ease. On the other hand, the multielectron reduction of CO_2 can give stable and useful products with much lower energies, as shown in Reference [3]. However, one photon can usually induce the transfer of only one electron in photochemical reactions. Overcoming this obstacle is a key goal in the design of efficient photocatalysts for CO_2 reduction.

$$CO_2 + e^- \rightarrow CO_2^{\bullet -}, \quad E^0 = -1.90\ \text{V} \tag{9.1}$$

$$CO_2 + 2H^+ + 2e^- \rightarrow CO + H_2O, \quad E^0 = -0.53\ \text{V} \tag{9.2}$$

$$CO_2 + 2H^+ + 2e^- \rightarrow HCO_2H, \quad E^0 = -0.61\ \text{V} \tag{9.3}$$

$$CO_2 + 4H^+ + 4e^- \rightarrow HCHO + H_2O, \quad E^0 = -0.48\ \text{V} \tag{9.4}$$

$$CO_2 + 6H^+ + 6e^- \rightarrow CH_3OH + H_2O, \quad E^0 = -0.38\ \text{V} \tag{9.5}$$

$$CO_2 + 8H^+ + 8e^- \rightarrow CH_4 + 2H_2O, \quad E^0 = -0.24\ \text{V} \tag{9.6}$$

There are several ways to reduce CO_2 with the assistance of renewable solar energy, and these methods can be divided into three major categories: homogeneous photoreduction by a molecular catalyst, photoelectrochemical reduction by a semiconducting photocathode, and electrochemical reduction by an electrolyzer powered by commercial photovoltaic (PV) devices.

9.1.2 Homogeneous Photocatalytic Reduction of CO_2

A homogeneous CO_2 photoreduction system consists of a molecular catalyst, light absorption, sacrificial electron donor, and/or electron relay. When looking at these types of systems, the main figure of merit is the photochemical quantum yield, defined as

$$\text{Photochemical quantum yield } (\text{Ø}) = \left(\frac{\text{moles products}}{\text{absorbed photons}} \right) \times (\text{number of electrons needed for conversion})$$

The generic mechanism of the photocatalytic reduction of CO_2 consists of a photosensitizer (P) capable of absorbing radiation in the ultraviolet (UV) or visible region and of the generation of an excited state (P*). The excited state is reductively quenched by a sacrificial donor (D) generating a singly reduced photosensitizer (P–) and oxidized donor (D+). The choice of photosensitizer must be such that P– is able to transfer an electron efficiently to the catalyst species (cat) to generate the reduced catalyst species (cat^-). In some cases, the photosensitizer and the catalyst are the same species. The cat^- is then able to bind CO_2 and proceed with the catalytic mechanism to release the intended products and regenerate cat. Common photosensitizers used in these systems include aromatics, *p*-terphenyl, phenazine, and polypyridine-coordinated transition metal complexes. The most common catalyst species include macrocycle complexes of Ni and Co, polypyridine Ru and Re catalysts, and suspended metal colloids.

Such metallomacrocycles strongly absorb visible light and do not require the addition of a photosensitizer. These systems do, however, suffer from low and low catalytic selectivity (CS) due to significant production of H_2. Tetraazamacrocyclics such as Ni(cyclam) have proved to reduce CO_2 efficiently and selectively to CO electrocatalytically while adsorbed on an Hg electrode. In purely photocatalytic systems, however, they tend to suffer from low CS and turnover number (TON). When Co is used as the metal center, the photocatalytic properties are improved. A well-studied catalyst, $Re(bipy)(CO)_3X$ (where bipy = 2,2-bipyridine and X = Cl, Br), capable of selective production of CO without the use of a separate photosensitizer was developed by Lehn and coworkers [4,5]. With the addition of phosphate groups to the $Re(bipy)(CO)_3X$ system ($X = P(OEt)_3$), one of the highest single-molecule quantum efficiencies was used for a homogeneous photocatalytic system. In a two-molecule system consisting of a 25:1 mixture of $Re(bipy)(CO)_3(P(OMe)_3)$ as a photosensitizer and $Re(bipy)(CO)_3MeCN$ as a catalyst, even higher quantum yields were achieved [6]. Although the Re catalyst systems mentioned above demonstrated remarkable, they lacked extended absorption in the visible region. With the use of solar photons, Ishitani and coworkers have addressed this issue by utilizing a bridging ligand to covalently attach a $[Ru(bipy)_3]^{2+}$-type photosensitizer, which absorbs strongly in the visible region, to a $Re(bipy)(CO)_3X$-type catalyst to create a supramolecular dyad complex.

Although photocatalytic reduction of CO_2 may become an important stepping stone to solar fuel production, much progress remains before it becomes practical as an industrial process. Currently, TONs remain in the hundreds and TOFs are

typically in the tens per hour. More mechanistic work must be done in order to understand and increase the stability and rates of these systems. These quantitative measures of catalytic systems must also be scrutinized because they are dependent on catalyst concentration and can vary drastically depending on the concentrations and volumes chosen for the experiment. To compound the problem, different solvents, electron donors, photosensitizers, and light sources are employed by the various groups studying these photocatalysts.

Looking forward to improved systems with a more practical utility, some additional issues are considered. As many of the photocatalysts presently studied are metal complexes employing rare and expensive transition metals, it is especially important to raise the catalytic rate and long-term stability to make this process economically feasible. Another drawback to the reviewed systems is the use of a sacrificial donor to supply the electrons for the reduction process. Ideally, water would be the source of both the electrons and hydrogen atoms for CO_2 reduction catalysis in an artificial photosynthetic process. These issues are not trivial and will take considerable effort and creativity to solve.

9.1.3 Heterogeneous Photoelectrochemical Reduction of CO_2

In a heterogeneous system, p-type semiconductor/liquid junctions are extensively studied as PV devices. The p-type semiconducting electrodes can act as photocathodes for photoassisted CO_2 reduction. Normally, there are four different types of photoassisted reduction of CO_2 using a semiconducting photocathode: (a) direct heterogeneous CO_2 reduction by a biased semiconductor photocathode, (b) heterogeneous CO_2 reduction by metal particles on a biased semiconductor photocathode, (c) homogeneous CO_2 reduction by a molecular catalyst through a semiconductor/molecular catalyst junction, and (d) heterogeneous CO_2 reduction by a molecular catalyst attached to the semiconductor photocathode surface [7–10].

Heterogeneous PEC reduction of CO_2 on semiconductor surfaces has been explored extensively in the last three decades. Both aqueous and nonaqueous solvents have been used for direct CO_2 PEC reduction on semiconductor surfaces, with the most commonly reported nonaqueous solvents being polypropylene carbonate, acetonitrile, dimethylformamide (DMF), dimethyl sulfoxide (DMSO), and methanol. The greatest difference between water and nonaqueous solvents is the solubility of CO_2. In nonaqueous solvents, the solubility is 7–8 times higher than in water. Methanol, for example, is known to be a physical absorber of CO_2 and is presently used in the rectisol processing industrial plants. Aqueous media further complicate CO_2 reduction, as different CO_2 hydration products are present in water. In water, CO_2 hydration occurs to form carbonic acid, which then undergoes stepwise dissociation to bicarbonate (HCO^{3-}) and carbonate (CO_2^{3-}). The predominant species is pH dependent: CO_2 is dominant at pH < 4.5; HCO^{3-} is dominant at 7.5 < pH < 8.5; and CO_2^{3-} is dominant at pH > 11.5. This, in turn, affects the thermodynamic potentials for generating certain products, as they are dependent on the form of CO_2 present in the solution.

Water, however, is commonly used as a proton source in aprotic solvents for CO_2 reduction. In one study, CO_2 solubility was shown not to change with the addition of up to 1% (500 mM) water to acetonitrile, but drastically decreased with higher water

concentrations. DMF and DMSO performed better than polypropylene carbonate and acetonitrile when mixed with 1% water, as they were better able to suppress competing proton reduction processes.

The limitations of CO_2 solubility in water at standard pressures as well as its diffusion limitations set a maximum catalytic current density of 10 mA cm^{-2} for electrochemical reduction of CO_2. CO_2 solubility, and thus maximum catalytic current, can be increased using high-pressure CO_2 environments. High-pressure CO_2 environments offer high catalytic current density and high selectivity over proton reduction for both metal and semiconductor electrodes. Gas-diffusion electrodes as well as other options have also been explored to increase CO_2 concentration, which is imperative to increase catalytic current densities.

Several metal electrodes have been used for catalytic reduction of CO_2 in both aqueous and nonaqueous media. The catalytic activity of a metal catalyst can be transferred to semiconductor photocathodes through discontinuous films of metals without sacrificing photovoltage. The objective of this approach is to incorporate the stability and catalytic activity of metal particles with semiconducting photocathodes. In a truly photoelectrocatalytic system, when a photoelectrode coupled to a catalyst (metal particles) is run under illumination, the Faradaic effciency (FE) versus applied potential has similar behavior to the catalyst alone with a positive shift in the onset voltage called the photovoltage shift. Apart from the photovoltage shift, catalytic activity and product distribution should not be affected by illumination.

On account of competing advantages of homogeneous catalysts (selectivity, tunability) and heterogeneous catalysts (robustness, easy separation of products from catalysts), there is considerable interest in "heterogenizing" homogeneous catalysts, by covalently linking them to surfaces. There have been several reports regarding surface modification of dark electrodes using the polymeric form of the molecular catalysts and/or enzymes for electrochemical reduction of CO_2 to various products. These modified dark electrodes have several advantages: control over the active site environment for better performance; prevention of aggregation or dimerization of the molecular catalyst, which leads to higher TONs; efficient charge transfer to the molecular catalyst; usability of water-insoluble molecular catalysts in aqueous media once anchored to electrodes; and stabilization of the catalyst and electrode [11,12]. The physical nature of these junctions is similar to a semiconductor/liquid junction with unbound molecular electrocatalysts [13]. Molecular catalyst surface-modified semiconductors can be subdivided into two categories: polymeric backbone attachment and direct anchoring to the semiconductor surface.

9.1.4 Prospect

Multijunction photoelectrolysis cells are presently used to overcome the high potential that is associated with water splitting. Four types of these cells are currently used: p/n junction photoelectrolysis cells, photoanode–PV cells, photocathode–PV cells, and PV photoelectrolysis cells.

Of note, the PV photoelectrolysis cell has a photovoltage that is independent of pH, which is important for pH-sensitive catalyst-mediated CO_2 reduction. This cell can also be easily modified with CO_2 reduction catalysts selective for specific

products. In addition, this type of cell utilizes a majority of the solar spectra and has a high photovoltage, unlike wide band gap semiconductor photoelectrodes. It is possible for this technology to be used as a wireless, monolithic, two-compartment PV-type photoelectrolysis cell with single dual-face photoelectrode. The fabrication cost of the electrode may be high; however, the simple structure of the cell, the ease of product separation, and the robustness of the electrode could lead to a long operation time and an environmentally friendly process. There are two major challenges for these types of cells: identifying catalysts based on earth-abundant materials that have low overpotentials for CO_2 reduction and water oxidation, and finding a reliable and robust proton-exchange membrane. It is clear that the advantages of this type of system outweigh the cost. Therefore, it is imperative to explore and adopt water-splitting/hydrogen-generation technology for solar splitting of CO_2 for liquid fuel applications as well as to broaden the search for new robust, selective, and efficient catalytic systems. In the quest for new catalysts, combinatorial approaches will prove useful for both discovery and optimization of new catalysts.

9.2 CATALYSTS FOR PHOTOELECTROCATALYTIC SYSTEM

9.2.1 Introduction

The transformation of CO_2 into fuel by using solar light irradiation is an effective method because there is no addition of extra energy and no negative influence on the environment. The immediate requirement in this technology is to develop visible light-sensitive photocatalysts, which are prominent in CO_2 recycling. Different types of photocatalysts have been already introduced by many researchers in this technology. Some of the catalysts exhibited high conversion rates and selectivity under visible light irradiation, whereas other catalysts were not feasible for visible light response and presented low yield rates. The reaction mechanism of selective photocatalysts under light irradiation is illustrated in Figure 9.1. Researchers are still trying hard to advance the properties of catalysts in terms of solar fuel production. A concise classification of photocatalysts is also shown in Figure 9.2, based on the recent development in photocatalytic CO_2 transformation.

9.2.2 Metal Oxide Photocatalysts

Metal oxides as light-sensitive catalysts have been applied in several processes such as the breaking down of organic and inorganic materials to valuable products, water treatment, and self-cleaning processes. The leading approach of using metal oxide catalysts in CO_2 conversion to carbonaceous fuel was introduced by Inoue et al. [15] Variations in metal oxide photocatalysts have already been introduced by integrating foreign elements and other compounds with different supportive substrates [16–19] for lessening its particle size, controlling its crystal growth, and increasing its surface area and pore volume. Various metal oxide photocatalysts, which were frequently studied in many photocatalytic CO_2 reduction processes, are characterized in this section. A clear idea of metal oxide semiconductors used in various studies for photocatalytic CO_2 transformation is represented in Table 9.1.

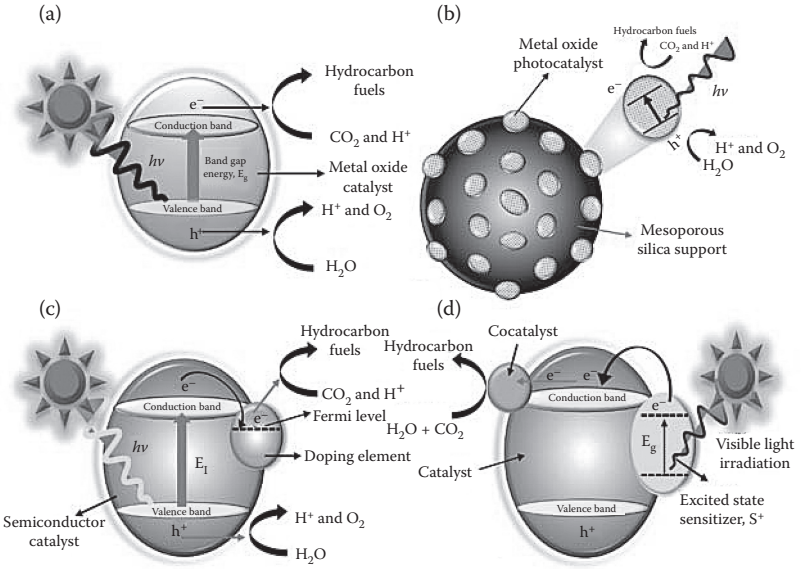

FIGURE 9.1 Photocatalytic reaction mechanism of (a) an unmodified metal oxide semiconductor; (b) supported metal oxide semiconductor; (c) doped semiconductor; and (d) dye-sensitized semiconductor under light irradiation. (Reprinted by permission from Macmillan Publishers Ltd. *RSC Adv.*, Das S, Daud WMA. A review on advances in photocatalysts towards CO_2 conversion, 4, 20856–20893, copyright 2014.)

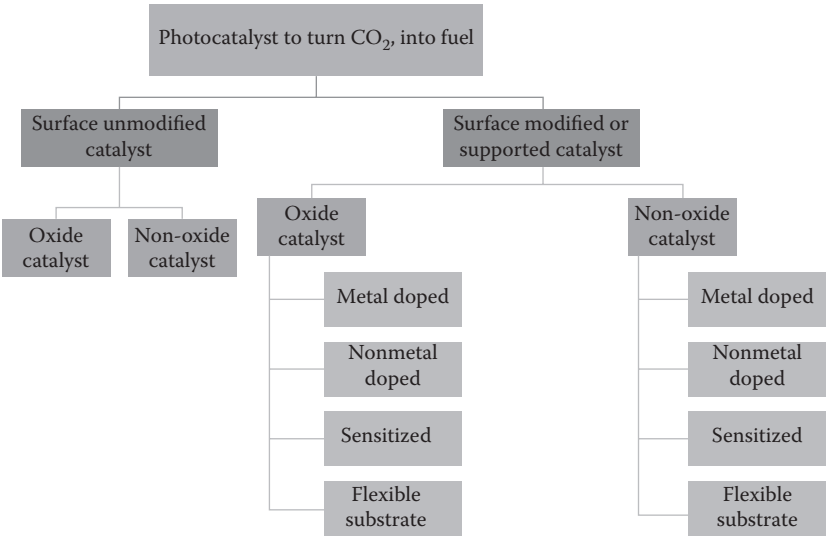

FIGURE 9.2 Classification of photocatalysts on CO_2 transformation into fuel. (Reprinted by permission from Macmillan Publishers Ltd. *RSC Adv.*, Das S, Daud WMA. A review on advances in photocatalysts towards CO_2 conversion, 4, 20856–20893, copyright 2014.)

TABLE 9.1
CO_2 Reduction Products and Corresponding Reduction Potential with Reference to NHE at pH 7

Product	Reaction	E^0_{redox} (V vs. NHE)
Oxygen	$H_2O \rightarrow 0.5O_2 + 2H^+ + 2e^-$	0.82
Methane	$CO_2 + 8H^+ + 8e^- \rightarrow CH_4 + 2H_2O$	–0.24
Ethane	$2CO_2 + 14H^+ + 14e^- \rightarrow C_2H_6 + 4H_2O$	–0.27
Carbon monoxide	$CO_2 + 2H^+ + 2e^- \rightarrow CO + H_2O$	–0.51
Methanol	$CO_2 + 6H^+ + 6e^- \rightarrow CH_3OH + H_2O$	–0.39
Ethanol	$2CO_2 + 12H^+ + 12e^- \rightarrow C_2H_5OH + 3H_2O$	–0.33
1-Propanol	$3CO_2 + 18H^+ + 18e^- \rightarrow CH_3CH_2CH_2OH + 5H_2O$	–0.31
2-Propanol	$3CO_2 + 18H^+ + 18e^- \rightarrow CH_3CH(OH)CH_3 + 5H_2O$	–0.30
Formaldehyde	$CO_2 + 4H^+ + 4e^- \rightarrow HCHO + H_2O$	–0.55
Acetaldehyde	$2CO_2 + 10H^+ + 10e^- \rightarrow CH_3CHO + 3H_2O$	–0.36
Propionaldehyde	$3CO_2 + 16H^+ + 16e^- \rightarrow CH_3CH_2CHO + 5H_2O$	–0.32
Acetone	$3CO_2 + 16H^+ + 16e^- \rightarrow CH_3COCH_3 + 5H_2O$	–0.31
Formic acid	$CO_2 + 2H^+ + 2e^- \rightarrow HCOOH$	–0.58
Acetic acid	$2CO_2 + 8H^+ + 8e^- \rightarrow CH_3COOH + 2H_2O$	–0.31

Source: Reprinted with permission from Hong J, Zhang W, Ren J, Xu R. Photocatalytic reduction of CO_2: A brief review on product analysis and systematic methods. *Anal. Methods*, 5, 1086–1097. Copyright 2013 American Chemical Society.

Being an inert, corrosion-resistant, and inexpensive semiconductor, TiO_2 is a frequently used metal oxide in the photocatalytic transformation of CO_2 into hydrocarbon fuel. In nature, TiO_2 is established as three familiar minerals such as rutile, anatase, and brookite. Among them, rutile and anatase phases indicate better efficiency under light radiation. Mutually, anatase and rutile phases reveal definite band gap energy at around 3.2 and 3.0 eV, respectively. The rutile phase is capable of absorbing visible light because of its comparatively low band gap energy, whereas the anatase form only displays its response to UV irradiation. Thus, the rutile phase is not used due to its ineffective photoactivity; the best photoactivity can be achieved by combining anatase with a slight amount of rutile. The light absorption by a TiO_2 semiconductor is effective, whereas the semiconductor exhibits high surface area. The surface area of TiO_2 is indirectly proportional to the size of particle; conversely, the size of the particle is directly proportional to the band gap energy. The semiconductor shows high band gap energy as a result of the shifting of valence band energy to lower energies after a certain decrease in the particle size, whereas band energy is intensely shifted to higher energies. On the other hand, significantly narrow band gap energy leads to inadequate redox potential to achieve oxidizing and reducing reactions. Therefore, it is compulsory to fix a structure that exhibits a settlement between the particle size and band gap energy range. Tan et al. investigated a combination of 80% anatase and 20% rutile forms as a photoactive catalyst [20]. Commercial Degussa P25 is found to be slightly less active than

modified TiO_2 (anatase and rutile) [21]. It is indicated that unmodified TiO_2 (P25) metal oxide semiconductors generally have high surface area as well as an affinity to organic impurities on their surfaces to facilitate the adsorption of organic compounds, which have the potential to perform as both an electron donor and a carbon source for the products [22]. Besides, this type of metal oxide catalyst expresses better methane production, compared with the Degussa P25 treated by calcination and washing where CO is the major product. In various studies, product dissimilarity is also observed due to the treatment procedure on anatase TiO_2 in several methods [23–25]. For instance, treatment by the acidic solutions (1 M nitric acid) is suitable for formic acid (FA) formation due to the protonation of reaction intermediates into the reaction medium. Treatment with 2-propanol acts as a hole scavenger in CO_2 photoreduction with anatase TiO_2, where the methane formation rate was considerably higher. Moreover, the synthesis of TiO_2 by the sol–gel method removes the presence of small brookite nanoparticles that normally arise in low-temperature formation reactions and considerably hinder the phase alteration to rutile at elevated temperatures.

Some prospective metal oxide photocatalysts other than TiO_2 were reported in many investigations. Inoue et al. studied three metal oxides, TiO_2, ZnO, and WO_3, to understand their photocatalytic characteristics under UV light radiation [15]. It was found that the yield of methyl alcohol increased as the conduction band becomes more negative with respect to the redox potential of H_2CO_3/CH_3OH, whereas methyl alcohol was not produced in the presence of WO_3 catalyst, which has a conduction band more positive than the redox potential of H_2CO_3/CH_3OH. However, WO_3 possesses low band gap energy (2.8 eV) with respect to visible light. $W_{18}O_{49}$ catalysts were synthesized in the form of nanowires with band gap energy of 2.7 eV for the photocatalytic conversion of CO_2 to methane under visible light irradiation. The diameter of $W_{18}O_{49}$ nanowires is approximately 0.9 nm and holds a large number of oxygen vacancies. These oxygen vacancies indicate an outstanding competency on photochemical carbon dioxide reduction over the visible light region.

Metal oxides such as Ga_2O_3, ZrO_2, and MgO were reported in various studies as having wide band gaps, compared with other photocatalytic metal oxides. In those studies, methane and hydrogen were used as reductants for photoreduction of CO_2, and CO was the major product. It was also observed that the surface bidentate formate species showed high photoactivity for photocatalytic reduction of CO_2 over ZrO_2 and MgO.

Recently, visible light-responsive and other oxide catalysts fabricated through various routes such as hydrothermal, solvothermal, and solid state reactions are widely used in the photochemical reduction of CO_2 because of high yield rates. It has been reported that hydrothermally prepared KNb_3O_8 and HNb_3O_8 nanobelts show high yields of methane, compared with the same catalysts derived from conventional solid state reactions and commercial TiO_2 (Degussa P25). In the case of hydrothermal synthesis, this nanobelt-like morphology and protonic acidity give higher photochemical activity for methane production through hydrogen bonding, which is facilitated by the separating and trapping of photogenerated carriers at the interlayer surfaces of HNb_3O_8 and KNb_3O_8. Ferroelectric materials can be used as remarkable substitutes for the standard semiconductor photocatalysts. Ferroelectric characteristics

lead to driving the electrons and holes apart because they possess internal dipoles. Therefore, this phenomenon decreases the probabilities of the recombination of carriers and also inhibits the reaction of redox products, driving the equilibrium toward product formation. For this ferroelectric behavior, the polar compound $LiNbO_3$ was used by Stock and Dunn for photocatalytic CO_2 conversion to FA under an Hg lamp or direct natural sunlight irradiation [26].

9.2.3 Modified/Unmodified Non-Oxide Catalysts

Non-oxide semiconductor photocatalysts are selected for CO_2 recycling because of their low band gap energy to facilitate the photocatalytic response to the visible light region, and high conversion efficiency is achieved for their unique photobehavior. It is investigated that semiconductor catalysts are one of the supreme sources for direct solar energy conversion. Many wide-ranging reviews already have been published on the advancement of oxide or non-oxide semiconductor photoactive materials. It was found that apart from the metal oxide semiconductor catalysts, metal sulfide semiconductor materials have effective photoactivity because of their outstanding ability to absorb the solar spectrum with high-energy yields [27]. Metal sulfides have comparatively high conduction band states more appropriate for enhanced solar responses than for metal oxide semiconductors, which are facilitated by the higher valence band states consisting of S 3p orbitals. It was reported that to absorb the entire UV and visible light region of solar irradiation, a $ZnS–AgInS_2–CuInS_2$ solid solution was capable due to an absorption edge of up to 800 nm. Cetyltrimethylammonium (CTA) with ZnS nanoparticles was used to inhibit the formation of bigger agglomerates. Different percentages of ZnS loading on porous SiO_2 matrices were also applied to investigate the improved photocatalytic yields. Cd–ZnS shows the highest activity than that of ZnS–CdS because Cd is more active in improving the quantum efficiency of the photochemical reduction of formate due to its ability to activate CO_2 more effectively in the photoreaction. Because of low band gap energy (3.0 eV) under the solar spectrum more competently, MnS semiconductor materials also have the distinct behavior of containing high reducing conduction band electrons which are satisfactorily active for encouraging the reduction of CO_2. That is why MnS semiconductors deliver higher quantum efficiency than other common catalysts such as TiO_2.

The use of catalysts for photochemical purposes without incorporating cocatalysts such as p-type GaP and p-type InP have also been studied due to narrow band gaps to facilitate the visible light response. Basically, in the PEC CO_2 conversion process, p-type metal phosphides (GaP) were mainly used in methanol production but needed remarkably high overpotentials. However, high faradaic efficiencies for the photoelectrochemical reduction of CO_2 to CO have also been investigated, whereas electrolytes are used in nonaqueous forms. Nevertheless, high overpotential is necessary to obtain high faradaic efficiency. It is found that p-type GaP was able to obtain faradaic efficiency of 100% while converting CO_2 to methanol at low potentials, which was more than 300 mV below the standard potential of 0.5 V versus the saturated calomel electrode (SCE). Furthermore, p-type GaP semiconductor exhibits low band gap energy (2.24 eV) and possesses high reducing conduction

band electrons to ease the reduction of CO_2. In another study, for CO_2 photocatalytic conversions, it was detected that p-type InP provided high selectivity for FA in a PEC cell.

9.3 PRODUCT AND SYSTEMATIC METHODS OF PHOTOCATALYTIC REDUCTION OF CO_2

9.3.1 Products of Photocatalytic Reduction of CO_2

Because of leads to possible climate change and a serious impact on globe environment, there is an increasing need to mitigate CO_2 emissions using carbon-neutral energy sources. CO_2 conversion includes chemical transformation, photocatalytic reduction, electrochemical reduction, biological conversion, etc. Among these, conversion of CO_2 to value-added fuels or chemical products by direct use of sunlight is an attractive but a challenging process. This certainly exerts stress in product identification and quantification. Hence, many groups have practically adopted the routine analysis of one or two products in either gas or liquid phase for evaluation of photocatalytic efficiencies.

CO_2 photoreduction involves multielectron processes which can lead to a large variety of products ranging from CO, CH_4 to higher hydrocarbons in the gas phase, and various oxygenates in the liquid phase such as alcohols, aldehydes, and carboxylic acids. A few representative reactions leading to gas and liquid products are shown in Table 9.1. The identification and quantification of such products are essential to more accurate evaluations of the photocatalytic performance of the designing of better photocatalysts.

9.3.2 Analysis of Gas-Phase Products

Scientists focused on the gas-phase product analysis for photocatalytic reduction of CO_2. One set of methods is proposed for the analysis of a wide range of photoreaction products in gas and liquid phases with low detection limits. The effects of the most commonly used organic additives were also investigated. Though the analysis methods discussed and proposed here are in the context of photocatalytic reduction of CO_2, they are also applicable for other CO_2 reduction processes, such as electrochemical reduction, chemical conversion, biological transformation, and so on. Furthermore, at the current stage of research, analysis techniques with low detection limits are also important to identify the influence of carbon residues originating from photocatalyst synthesis which can possibly contribute to the reduction products.

CH_4 and CO are the major gaseous products of CO_2 photoreduction, whereas H_2 and/or O_2 may also be produced as byproducts from water splitting. In addition, higher alkanes as the photocatalytic reduction products of CO_2 was observed. Besides the products, CO_2 as the main species in the gas phase due to a low conversion needs to be quantified to determine the reaction progress and/or the extent of CO_2 dissolution in the liquid phase. Infrared spectroscopy (IR) or diffuse reflectance infrared Fourier transform spectroscopy (DRIFT) has been occasionally employed

to verify the consumption of CO_2 and the generation of CO. Gas chromatography (GC) is by far the most commonly used method for quantification of these gas species. Besides GC, gas chromatography–mass spectroscopy (GC–MS) was also used for routine analysis of CH_4 and CO or for carbon source verification. Although a thermal conductivity detector (TCD) was the only detector used in GC as stated in some reports, it is suggested that a flame ionization detector (FID) should be used in order to achieve higher sensitivities for detection of low concentrations of CO and hydrocarbons. FID analysis is a destructive method. Therefore, the gas should first be analyzed by TCD for gases quantification followed by FID for the analysis of CO and alkanes. Many types of columns have been used, such as molecular sieves, carbon columns, and Al_2O_3. It has been noted that if a high concentration of CO_2 remains in the gas product stream, it can cause deactivation of the nickel catalyst in the methanizer and certain types of columns, including the most commonly used molecular sieve column, making frequent column regeneration necessary. Herein, a better design of GC configuration is proposed to separate and detect all the gases, including CH_4, CH_3CH_3, CO, CO_2, O_2, N_2, and H_2 with low detection limits as well as to avoid regular column regeneration and achieve longer lifetimes of the methanizer and detector.

Some research groups adopted the gas-phase reaction for CO_2 photoreduction. In a typical gas-phase reaction, the solid photocatalyst was initially well dispersed at the bottom of the reactor which contains CO_2 gas, followed by injecting a small amount of liquid water (e.g., 1 mL). Under a low-pressure condition, liquid water vaporizes and mixes with CO_2 gas. In these cases, the analysis methods proposed above can be used for accurate analysis of gas products. Gas-phase reduction was also carried out using H_2 or CH_4 instead of water to reduce CO_2. For these water-free gas–solid systems, a GC-based method is still widely used for the quantification of products. Nevertheless, it is worth noting that *in situ* DRIFT coupled with isotopically labeled $^{13}CO_2$ can be employed to monitor the intermediates or products adsorbed on the solid photocatalyst surface.

9.3.3 Analysis of Liquid-Phase Products

Although GC with TCD/FID is still the main technique used for the analysis of different types of liquid oxygenates (mainly alcohols), several other methods have been utilized, including GC–MS [29–31], high-performance liquid chromatography (HPLC), ion exchange chromatography (IEC), UV–visible (UV–Vis) spectroscopy (colorimetric assay) after reacting with chromotropic acid or Nash reagent, and nuclear magnetic resonance (NMR). The compounds that can be analyzed and their detection limits using various techniques, together with the associated limitations, are summarized in Table 9.2.

It is well known that alcohols (especially methanol) are frequently detected products from CO_2 photoreduction in the liquid phase. GC with an FID works well for the analysis of alcohols, and several kinds of columns have been used such as HP-5, DB-WAX, and polyethylene glycol (PEG) columns.

In many studies, organic compounds have been engaged in photoreduction of CO_2 for various reasons such as sacrificial reagents (e.g., methanol, triethanolamine),

TABLE 9.2
Comparison of Techniques Used for Liquid-Phase Analysis in CO_2 Photoreduction

Technique	Compounds	Detection Limit	Limitations
GC	Alcohols	3 μmol L^{-1}	Much higher detection limits for aldehydes
	Aldehydes	100 μmol L^{-1}	
HPLC	Carboxylic acids	5 μmol L^{-1}	Aldehydes need to be derivatized before analysis
	Aldehydes	0.07 μmol L^{-1}	
IEC	Carboxylic acids	0.1 μmol L^{-1} for HCOOH 10 μmol L^{-1} for CH_3COOH	For acids only
UV–Vis	HCHO after reaction with Nash's reagent or HCOOH	0.17 μmol L^{-1} 0.08 μmol L^{-1}	Not applicable for other aldehydes and acids; HCOOH can only be analyzed when no other organics are present
^1H or ^{13}C NMR	All oxygenates	Not available	High cost, difficult for quantification, although some work demonstrated quantification, mainly for product qualification, carbon source verification
GC/LC–MS	All oxygenates	Not available	Mainly for product qualification, carbon source verification

Source: Reprinted with permission from Hong J, Zhang W, Ren J, Xu R. Photocatalytic reduction of CO_2: A brief review on product analysis and systematic methods. *Anal. Methods*, 5, 1086–1097. Copyright 2013 American Chemical Society.

solvents (e.g., acetonitrile, DMF), photocatalysts (e.g., Ru complexes) or photosensitizers (e.g., N3 dye, Rose bengal). The presence of such organic compounds in the reaction systems may affect the product analysis in the liquid phase.

Another group of possible reduction products, aldehyde analytical techniques needs to be developed for CO_2 reduction product screening. Besides Nash's colorimetric method, others also used GC with either TCD/FID with a Porapak T column or FID with a DB-WAX column 30 and BX-10 column to quantify aldehydes. Hence, only relatively concentrated aldehydes can be analyzed by the GC method, whereas the concentrations of aldehydes in the liquid phase of CO_2 photoreduction are usually much lower than such detection limits.

9.3.4 Carbon Source Verification and O_2 Monitoring

The contribution of carbon residues to the photoreduction products has been recently reported [32]. The *in situ* DRIFT study indicated that ^{12}CO was the main product when $^{13}CO_2$ gas was used during surface photoreaction over the Cu(I)/TiO_2 catalyst.

The ^{12}C source was proven to be from the carbon residue on the photocatalyst, originating from the organics used during photocatalyst preparation. Based on this, the photocatalytic activities reported for CO_2 reduction in the literature may need to be verified if there was no tracking of carbon source or enough evidence for photocatalytic events. Thus, either carefully and systematically designed control experiments or carbon source tracking by NMR, GC–MS, or LC–MS with isotope ^{13}C-labeled CO_2 as the reactant, is necessary. The carbon source in gas products such as methane and carbon monoxide can be verified by spectroscopic methods (e.g., DRIFT) or GC–MS, and in liquid oxygenates by ^{13}C NMR, GC–MS, or LC–MS. For example, Liu et al. studied the solvent effect on photocatalytic CO_2 reduction by using $^{13}CO_2$ with GC–MS and ^{13}C NMR to identify the source of carbon in CO and liquid products, respectively [33]. Yui et al. reported the use of TiO_2 (P25) for methane production. The carbon source of methane was confirmed from CO_2 based on a signal at $m/z = 17$ ($^{13}CH_4$) in GC–MS when $^{13}CO_2$ was used [22]. The photocatalytic activity of a titanium metal–organic framework in CO_2 reduction to produce FA was confirmed by using ^{13}C NMR. A signal at 165.30 ppm can be found, which was assigned to HCOO, whereas such a signal was not found when $^{12}CO_2$ was used. In another report, ^{13}C-labeled HCOOH in the product was found to be easily detected by ^{13}C NMR, to confirm that the product was from the reduction of CO_2 rather than from other carbon sources on the used carbon nanoparticles. Using layered double hydroxides as a photocatalyst, the carbon source of CO and oxygen source of O_2 were also confirmed from CO_2 and H_2O, respectively, by using $^{13}CO_2$ and $H_2{}^{18}O$ with GC–MS method [34].

On the other hand, O_2 evolution is an important indicating factor to support photocatalytic CO_2 reduction, whereas water is used as the reducing agent for CO_2. Kudo and coworkers [35] reported that the production of H_2, O_2, and CO is stoichiometric over Ag-loaded $ALa_4Ti_4O_{15}$ (A = Ca, Sr, and Ba) photocatalysts. The ratio of the mole of reacted electrons to that of holes was found to be almost unity, indicating that the CO_2 reduction occurred photocatalytically with water as the reducing agent. To ascertain that O_2 is generated from the reaction rather than from air contamination, the volumetric (molar) ratio of O_2 to N_2 over reaction time should be monitored. In a recent study, the molar ratio of O_2/N_2 was found to gradually increase from 0.26 (the ratio in air) to 0.40 after light irradiation. In addition, the trend of this ratio was found to be similar to that of CH_4 production, indicating that O_2 was produced by photoreaction (see Figure 9.3).

In summary, major products in both gas and liquid phases from CO_2 photoreduction can be detected accurately with low detection limits by a combination of GC and HPLC methods. Figure 8.3 summarizes the analysis methods and the detection limits of the major chemical species in both gas and liquid phases in the absence of organic additives. The effects of several organic additives, including commonly used solvents, photosensitizers, and sacrificial reagents, in photoreaction were investigated. It has been found that alcohol analysis by GC methods is more sensitive to organic additives, whereas aldehyde and acid analyses by HPLC methods are not affected by most of the organics investigated. The importance of carbon source verification is highlighted and several techniques such as DRIFT, NMR, and GC–MS can be used.

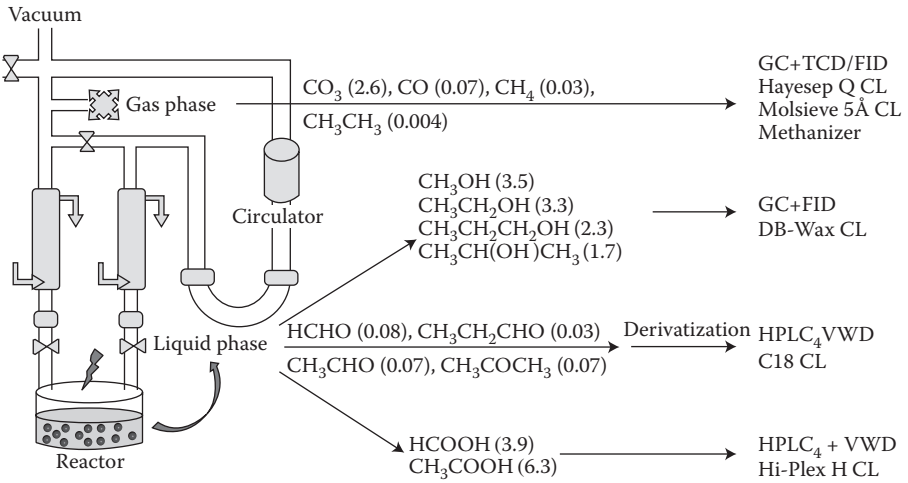

FIGURE 9.3 Summary of analysis methods for gas and liquid-phase samples. Derivatization: aldehydes were derivatized with DNPH before performing HPLC analysis. The detection limits (μmol L^{-1}) are shown in brackets. (Reprinted by permission from Hong J, Zhang W, Ren J, Xu R. Photocatalytic reduction of CO_2: A brief review on product analysis and systematic methods. *Anal. Methods*, 5, 1086–1097. Copyright 2013 American Chemical Society.)

9.4 CONVERSION OF CARBON DIOXIDE INTO METHANOL

9.4.1 Potential Advantages of Converting CO_2 into Methanol

At present, most of the commercial methanol is produced from synthetic gas (also called as syngas, which is a mixture of CO and H_2) on quite large-scale industrial plants in several millions tons per year capacity. Besides this, the processes such as selective oxidation of methane, catalytic gas-phase oxidation of methane, liquid-phase oxidation of methane, monohalogenation of methane, microbial and photochemical conversion of methane, etc. are also being employed to produce methanol. Nevertheless, production of methanol from CO_2 using solar energy to drive the reaction is highly attractive as it saves the natural fossil fuel resources.

Converting CO_2 into value-added chemicals, such as methanol, is both challenging and rewarding. The conversion of CO_2 into methanol using energy has been suggested to be one of the best ways of storing energy and solving both global warming and energy crisis problems to a great extent. The additional advantages in producing methanol from CO_2 include (i) high energy density by volume and by weight; (ii) no need of high pressures to store at room temperature like H_2 needs; (iii) relatively low toxic and safe to handle fuel, and shows limited risks in its distribution (non-technical); (iv) no need to modify the internal combustion engines of the vehicles to use methanol; and (v) no impact on the environment during production and usage as methanol being a primary feedstock for many of the organic compounds, and a vital intermediate for several bulk chemicals used in day-to-day life products such

as silicone, paint, and plastics. Furthermore, methanol is a green fuel and has almost half of the energy density in comparison to the mostly used fuel, gasoline (methanol: 15.6 MJ/L; gasoline: 34.2 MJ/L), also be employed directly in the fuel cells.

The methanol economy and uses of methanol conversion from CO_2 have been largely discussed, whereas an economy based on FA has been proposed by Ferenc [35]. However, the formation of renewable H_2 is the key step in the conversion of CO_2 into methanol, and there are already certain established technologies for producing H_2 from water (a carbon-neutral resource) using electricity. Based on several factors as discussed in several published review articles, the PV/electrolyzer approach shows unmatched potential for the CO_2 catalytic hydrogenation route. However, the biochemical, thermochemical, and PEC splitting of water into hydrogen would show better results if these processes are directly integrated with the CO_2 reduction reaction in comparison to the PV/electrolyzer-based process, where H_2 needs to be produced separately and then used for reducing CO_2 in a separate process.

9.4.2 Photoelectrochemical Reduction of CO_2 into Methanol

Methanol can be prepared from CO_2 by catalytic hydrogenation and dehydration. These two reactions can also be performed together in a single step. All these reactions are equilibrium reactions, they occur almost at the same temperature and on the same catalyst. Table 9.3 lists the various catalytic systems employed for synthesis of methanol from CO_2 by following catalytic hydrogenation (i.e., thermochemical) routes [36,37]. In fact, the synthesis of methanol from syngas over copper–zinc oxide-based catalysts is a well-established process, and about 40 M tons of methanol per year is being produced every year at present by following this route. In this commercial process, about 3% CO_2 is supplied together with syngas to enhance the reaction rate. Because reverse water–gas shift (RWGS) is a reversible reaction, the same catalyst can be employed to carry out both reactions of water–gas shift (WGS) and RWGS. The best catalyst noted for these reactions has been a multicomponent Cu/$ZnO/ZrO_2/Al_2O_3/SiO_2$ composition.

From the above, it can be understood that the activity of direct formation of methanol by the catalytic hydrogenation of CO_2 is not only influenced by active catalytic sites but also by the support material. The Cu supported on CuO/ZnO with 30/70 weight ratio provided a methanol yield of 3.63×10^{-5} kg per square meter of the catalyst per hour at 250°C under a pressure of 75 atm., whereas pure Cu provided a yield of less than 10^{-8} kg per square meter of the catalyst per hour [38]. According to a theory, addition of wurtzite ZnO with an n-type semiconductor to Cu/CuO catalysts creates cation and anion lattice vacancies, which are responsible for improved adsorption and transformation of CO_2 as well as the enhancement of Cu dispersion on the catalyst support. The formate intermediate was found to adsorb at the interface between Cu and ZnO or Cu–O–Zn. By employing the mixtures of Cu/SiO_2 + ZnO/SiO_2 as catalysts, it was found that ZnO creates Cu–Zn active sites for this reaction, and the morphology of Cu was found to undergo any change during the reaction. Further, ZnO is believed to stabilize many active sites by absorbing the impurities present in the syngas stream. A small amount of sulfur could be a poison

TABLE 9.3
Catalysts Employed in the Catalytic Hydrogenation of CO_2 into Methanol

Catalyst	Catalyst Preparation Method	Reaction Temperature (°C)	CO_2 Conversion (%)	Methanol Selectivity (%)	Methanol Activity (mol kg^{-1} cat. h)
$Cu/Zn/Ga/SiO_2$	Co-impregnation	270	5.6	99.5	10.9
Cu/Ga/ZnO	Co-impregnation	270	6.0	88.0	11.8
Cu/ZrO_2	Deposition–precipitation	240	6.3	48.8	11.2
$Cu/Ga/ZrO_2$	Deposition–precipitation	250	13.7	75.5	1.9
$Cu/B/ZrO_2$	Deposition–precipitation	250	15.8	67.2	1.8
$Cu/Zn/Ga/ZrO_2$	Coprecipitation	250	n/a	75.0	10.1
$Cu/Zn/ZrO_2$	Coprecipitation	250	19.4	29.3	n/a
$Cu/Zn/ZrO_2$	Urea–nitrate combustion	240	17.0	56.2	n/a
$Cu/Zn/ZrO_2$	Coprecipitation	220	21.0	68.0	5.6
$Cu/Zn/ZrO_2$	Glycine–nitrate combustion	220	12.0	71.1	n/a
$Cu/Zn/Al/ZrO_2$	Coprecipitation	240	18.7	47.2	n/a
$Ag/Zn/ZrO_2$	Coprecipitation	220	2.0	97.0	0.46
$Au/Zn/ZrO_2$	Coprecipitation	220	1.5	100	0.40
$Pd/Zn/ZrO_2$	Incipient wetness	250	6.3	99.6	1.1
Ga_2O_3–Pd/SiO_2	Incipient wetness	250	n/a	70.0	7.9
$LaCr_{0.5}Cu_{0.5}O_3$	Sol–gel	250	10.4	90.8	n/a

Source: Reprinted by permission from Macmillan Publishers Ltd. *Renew. Sust. Energ. Rev.*, Ganesh I. Conversion of carbon dioxide into methanol—a potential liquid fuel: Fundamental challenges and opportunities (a review), 31, 221–257, copyright 2014.

for Cu catalyst if ZnO is absent as a support, thus ZnO inhibits the sulfur poisoning of Cu active sites during this reaction.

The reaction activity, product yield, and catalyst life are not only found to be by the catalyst composition but also by the reaction conditions employed. As both catalytic hydrogenations of CO and CO_2 into methanol are exothermic reactions, methanol conversion was found to be increased upon increasing the reaction pressure and decreasing the reaction temperature according to the Le Chartelier's principle. As the equilibrium constant decreases with an increase in temperature, a low-temperature condition is preferred for methanol formation. However, increasing reaction temperature could also increase the reaction rates for both these hydrogenation reactions. Nevertheless, methanol formation has been found to be sensitive to optimal temperature ranges over different catalysts. Higher reaction temperatures could also rapidly reduce the activity and shorten the catalyst lifetime by promoting the sintering process and agglomeration of Cu on the catalyst surface. Catalysts also tend to undergo deactivation faster at high pressures again by the enhanced sintering process. A search for an ideal catalyst system that is very active under low pressures and low temperatures with long lifetime is still active.

In PEC cells, the semiconductor electrode immersed in the electrolyte is connected through an external circuit to a counter electrode. When this semiconductor electrode is illuminated by any light that is having energy higher than the band gap of this semiconductor, its electrons excite from the valance band to conduction band, and reach cathode counter electrode through an external wire. Furthermore, the electron–hole pairs thus formed are spatially separated by the semiconductor junction barrier, and are injected into the electrolyte at the respective electrodes to produce electrochemical oxidation and reduction reactions. As of now, not even a single semiconducting material has been identified which can be employed as a photoelectrode to split water into hydrogen and oxygen gases or reduce CO_2 into methanol using exclusively solar energy in an aqueous-based PEC cell with desired stability and efficiency. However, it needs greater energy input to make up losses due to band bending (necessary in order to separate charge at the semiconductor surface), resistance losses, and overvoltage potentials. When a semiconductor is placed in an electrolyte, partial differences between the two phases result in charging of the interface. This charging results in a perturbation of the energy levels of the semiconductor called "band-bending." Band bending is responsible for separation of electron–hole pairs in PEC reactions. Recombination and corrosion processes decrease the utilization of the electron–hole pairs generated on illumination. A major impediment to the exploitation of PEC cells in solar energy conversion and storage is the susceptibility of small band gap semiconductor materials to photoanodic and photocathodic degradation. The photoinstability is particularly severe for n-type semiconductors where the photogenerated holes, which reach the interface, can oxidize the semiconductor material itself. In fact, many of the semiconducting materials are predicted to exhibit thermodynamic instability toward anodic photodegradation. Whether a photoelectrode is stable or not depends on the competitive rates of the thermodynamically possible reactions such as the semiconductor decomposition reaction and the electrolyte reactions.

9.4.3 Oxide Semiconductors as Cathode Materials

The photoreduction of CO_2 involves two main free radicals H and CO_2^{3-}, which are formed by taking electrons from photocathode (i.e., from semiconductor), when the electrons of this semiconductor are excited from the valence band to the conduction band by absorbing a photon having energy equal to or greater than that of the band gap of the semiconductor. TiO_2 being a very stable material against photocorrosion and possessing band edges amenable to water oxidation/electrolysis reaction, it has been considered as an ideal material to use in PEC reduction or photocatalytic reduction of CO_2. As the band gap energy of TiO_2 is high (3.2 eV), which is equivalent to UV light, it cannot capture a larger portion of sunlight; hence, the efficiency of the system involving pure TiO_2 photoelectrode does not exceed 4% as the percentage of UV light in the entire solar spectrum is only about 4%. Several researchers have tried to improve the light-absorbing capability of TiO_2 by doping it with several metals and nonmetals. For example, Cu was dispersed into an aqueous suspension of TiO_2 to enhance the photocatalytic activity and reduction of TiO_2 for reducing CO_2 into methanol [39–41]. Those distinct catalytic steps include (i) photoelectron–hole pair generation, charge separation, and trapping; (ii) oxidation and reduction reactions of the adsorbates; (iii) rearrangement and other surface reactions of formed intermediates; and (iv) the desorption of the products from the photocatalyst surface and the regeneration of the surface. The TiO_2 and TiO_2-supported Cu catalysts formed in a sol–gel route were also investigated for photocatalytic of CO_2.

Not only powder catalysts, but also the thin films of Cu-doped TiO_2, and Cu-containing zinc oxide surface-coated Pt electrodes were employed for photocatalytic CO_2 reduction reaction in an aqueous-based electrolyte [41–43]. The pulse technique has been used in a regular electrochemical reduction of CO_2 with a pair of Cu electrodes, which normally prevent the deactivation of hydrocarbon formation catalyst [44]. Furthermore, when the pulsed mode technique was employed to supply bias potential, the noted results were remarkable, and it increased the activity for methane and ethylene formation.

CO_2 was also reduced to methane, ethylene, and CO in CO_2-saturated aqueous electrolyte over the surface of illuminated p-Si semiconductor electrode surface modified with small metal particles of Cu, Ag, or Au [45]. These modified p-Si semiconductor electrodes produced products similar to the metal (Cu, Ag, or Au) electrodes, but at ca. 0.5 V (vs. NHE) more positive potentials than their corresponding metal electrodes, contrary to continuous metal-coated p-Si electrodes. These results clearly suggest that the metal-particle-coated p-Si electrodes not only possess high catalytic activity for electrode reactions, but also generate high photovoltages and thus work as ideal semiconductor electrodes. The formation of the dimeric and tetrameric products, namely oxalate, glyoxylate, glycolate, and tartrate, was also noted in the CO_2 reduction reaction when performed in an aqueous solution of tetramethylammonium chloride suspended with CdS or ZnS colloids. The performance of other semiconducting powders, including ZnO, SiC, $BaTiO_3$, and $SrTiO_3$, was also compared with those exhibited by CdS and ZnS colloids. The formation of HCOOH and HCHO was noted in the absence of tetramethylammonium ions. The relative quantum efficiencies of these semiconductors were found to be influenced by their

band gap energies and conduction band potentials. The role and effectiveness of several hole acceptor (electron donor) compounds in this process were also studied, and it was found that the addition of one electron to a CO_2 molecule produces a CO_2^{3-} radical anion. It can be concluded that the semiconductors, particularly CdS, SiC, and ZnS, with the higher negative conduction band potentials provide the best yields. Although the effectiveness of different semiconductors in reducing CO_2 is roughly in line with the order of increasing conduction band potentials, the variations, which are fairly small, may also be related to differences in particle size, which in quantum crystallites results in an increase in band gap and reduction in the rate of recombination of electron–hole pairs. The overall quantum yields exhibited by these six semiconductors followed this trend: ZnS > SiC > ZnO > CdS > $BaTiO_3$ > $SrTiO_3$.

From the above presented photocatalytic results, it can be concluded that although encouraging progress has been made toward the photocatalytic conversion of CO_2 using sunlight, further efforts are required for increasing sunlight-to-fuel photoconversion efficiencies.

9.4.4 Non-Oxide P-Type Semiconductors as Cathode Materials

In 1978, for the first time, a photoelectrode made of a single crystal p-gallium phosphide (p-GaP) was employed in a PEC cell for converting CO_2 into FA, formaldehyde, and methanol. Unlike the reduction of CO_2 on metal cathodes, which stops essentially after two electron transfers because of high overpotential associated with FA reduction, the photoelectrolysis on p-GaP proceeds further to yield formaldehyde and methanol. After 90 h of irradiation, the concentrations of FA, formaldehyde, and methanol formed were estimated to be 5×10^{-2}, 2.8×10^{-4}, and 8.1×10^{-4} M, respectively. In this process, the efficiency of the system was calculated using the formula suggested. Optical conversion efficiency is nothing but the efficiency of conversion of radiant energy into the chemical energy. The results clearly indicate that in contrast to the reduction of CO_2 on certain metal cathodes, the photoelectrolysis on p-GaP does not stop after FA formation, but proceeds further, yielding formaldehyde and methanol.

Subsequent to the above study, there were several studies aimed at reducing CO_2 into highly reduced products using different types of semiconducting materials in PEC cells [46]. As part of this, CO_2 was also reduced to methanol over n- and p-GaAs, n-Si, and p-InP semiconductors. Reduction at n-GaAs was found to be selective with nearly 100% Faradaic efficiency. However, these semiconductors are susceptible to corrosion. CO_2 was also reduced to HCOOH, HCHO, methanol, and CH_4 over various other semiconducting materials that include WO_3, TiO_2, ZnO, CdS, GaP, and SiC. HCHO and methanol were found to be the major products over SiC semiconductor catalyst after illumination for 7 h. The methanol yield was found to be increased as the conduction band becomes more negative with respect to the redox potential of H_2CO_3/methanol, whereas methanol was not produced at all in the presence of WO_3 catalyst that has a conduction band more positive than this redox potential. CO_2 was also found to be reduced electrocatalytically to HCOOH, HCHO, methanol, and CH_4 at unilluminated TiO_2 electrode or at the illuminated p-GaP electrode when both semiconductor electrodes were polarized at a potential of −1.5 V vs. SCE for 2 h, which indicates that electrons in the conduction bands of

these semiconductors reduce CO_2 in aqueous solution. It has been suggested that at semiconductor electrodes, the charge transfer rates between photogenerated carriers in semiconductors and the solution species depend on the correlation of energy levels between the semiconductor and the redox agents in the solution. If the redox potential of solution species is more positive with respect to the conduction band level, then these species undergo improved reduction.

CO_2 also underwent reduction over a biological catalyst (a formate dehydrogenase enzyme) in a PEC cell over the surface of p-InP illuminated with a light source having wavelength range shorter than 900 nm (>1.35 eV). This enzyme catalyst performs two electron reduction of CO_2 to FA with the help of a mediator that couples the photogenerated electrons in the semiconductor with the enzyme catalyst. Although this process appears to be more analogous to natural photosynthesis, the former process is more efficient at light collection and more specific in the production of reduced carbon species. Among the various reaction conditions, the CO_2 pressure was found to be very critical for obtaining higher product yields. When CO_2 reduction reaction was performed over p-GaP and p-GaAs semiconductors in a PEC autoclave fitted with a quartz window, a cation exchange diaphragm, and a platinum counter electrode under the illumination with a 150 W Xe lamp, the formation of HCOOH, HCHO, and methanol was noted with a Faradaic efficiency of 80% on the surface of p-GaP at a cathodic bias of –1.00 V (vs. a standard silver electrode) in 0.5 M Na_2CO_3 solution under 8.5 atm. CO_2 pressure [47,48].

Although by following PEC routes, CO_2 could be converted into methanol using certain non-oxide semiconducting photoelectrodes (p-GaP) together with homogeneous organic molecular catalysts (pyridine), the recorded quantum efficiencies and the stability and durability of these routes have been rather low and insufficient for practicing on a commercial scale. This is due to the fact that these routes still need certain amount of external bias voltage from grid current, and the associated semiconductors show poor long-term stability against photocorrosion being non-oxide materials.

Among the stoichiometric, thermochemical, electrochemical, PEC, and photocatalytic routes developed so far for reducing CO_2 into value-added chemicals, only the electrochemical routes appear to be viable as these latter routes allow mild reaction conditions, most studied and understood systems only next to the thermochemical processes, and can be integrated with electricity that is derived from sunlight using any of the existing technologies such as PVs. However, the reaction efficiencies and product yields obtained in these electrochemical routes are also low at the moment. Nevertheless, these reaction efficiencies and product yields could be improved suitably (i) by suppressing the hydrogen evolution reaction (HER), which is the main reason for the noted low efficiency of the process, by using certain electrodes having high overpotentials toward HER; (ii) by reducing overpotentials associated with CO_2 reduction reaction into methanol using suitable molecular catalysts, such as room temperature ionic liquids (RTILs), pyridine, and a mixture of nitroso-R salt+Co or Cu sulfate+methanol, which can be employed in conjunction with electrodes; and (iii) by employing electricity that is produced from sunlight using cheaper technologies such as polymer-based PVs. Furthermore, the HER could also be suppressed by using certain organic molecular catalysts, such as triethanolamine, in the anode compartment of the electrochemical reaction.

9.5 CONCLUSIONS AND OUTLOOK

Research in the field of photochemical and PEC reduction of CO_2 has grown rapidly now. It is a response by physical scientists and engineers to the increasing amount of CO_2 in the atmosphere and the steady growth in global fuel demand. CO_2 is an extremely stable molecule generally produced by fossil fuel combustion and respiration. Returning CO_2 to a useful state by activation/reduction is a challenging task in chemical catalysis, electrochemistry, photochemistry, and semiconductor physics and engineering.

PEC which uses both homogeneous and heterogeneous system for CO_2 reduction has been reviewed. In homogeneous systems, some photocatalysts using transition metal complexes show outstanding performance, such as high absorbance in the visible region, high quantum yields, and high product selectivities. CO_2 reduction using semiconductor photocatalysts, such as metal oxide semiconductors TiO_2, has been increasing rapidly. Organic contaminants have paid attention to both carbon sources and reductants of the reaction products for photocatalytic reduction of CO_2.

Development of an efficient process for converting CO_2 into methanol or to any other value-added chemical using exclusively solar energy is of great importance, as this process can indeed deal with (i) the CO_2-associated global warming problem, (ii) depletion of fossil fuels, and (iii) the problems associated with storing of energy (electricity as well as solar energy) in the form of high energy density liquid fuels for future applications.

REFERENCES

1. Kumar B, Llorente M, Froehlich J et al. Photochemical and photoelectrochemical reduction of CO_2. *Ann. Rev. Phys. Chem.*, 2012, 63, 541–569.
2. Kedzierzawski P, Augustynski J. Poisoning and activation of the gold cathode during electroreduction of CO_2. *J. Electrochem. Soc.*, 1994, 141, 58–60.
3. Saveant J-M. Molecular catalysis of electrochemical reactions: Mechanistic aspects. *Chem. Rev.*, 2008, 108, 2348–2378.
4. Hawecker J, Lehn J-M, Ziessel R. Efficient photochemical reduction of CO_2 to CO by visible light irradiation of systems containing Re(bipy)(CO)3X or Ru(bipy)32+ – CO_2+ combinations as homogeneous catalysts. *J. Chem. Soc. Chem. Commun.*, 1983, 9, 536–538.
5. Hawecker J, Lehn J-M, Ziessel R. Photochemical and electrochemical reduction of carbon dioxide to carbon monoxide mediated by (2,2'-bipyridine)tricarbonylchlororhenium(I) and related complexes as homogeneous catalysts. Helv. *Chim. Acta*, 1986, 69, 1990–2012.
6. Takeda H, Koike K, Inoue H, Ishitani O. Development of an efficient photocatalytic system for CO_2 reduction using rhenium(I) complexes based on mechanistic studies. *J. Am. Chem. Soc.*, 2008, 130, 2023–2031.
7. Bockris JOM, Wass JC. On the photoelectrocatalytic reduction of carbon dioxide. *Mater. Chem. Phys.*, 1989, 22, 249–280.
8. Junfu L, Baozhu C. Photoelectrochemical reduction of carbon dioxide on a p^+/p^-Si photocathode in aqueous electrolyte. *J. Electroanal. Chem.*, 1992, 324, 191–200.
9. Beley M, Collin J-P, Sauvage J-P, Petit J-P, Chartier P. Photoassisted electro-reduction of CO_2 on p-GaAs in the presence of Ni cyclam^{2+}. *J. Electroanal. Chem.*, 1986, 206, 333–339.

10. Aurian-Blajeni B, Taniguchi I, Bockris JOM. Photoelectrochemical reduction of carbon dioxideusing polyaniline-coated silicon. *J. Electroanal. Chem.*, 1983, 149, 291–293.
11. Dominey RN, Lewis NS, Bruce JA, Bookbinder DC, Wrighton MS. Improvement of photoelectrochemical hydrogen generation by surface modification of p-type silicon semiconductor photocathodes. *J. Am. Chem. Soc.*, 1982, 104, 467–482.
12. Lewis NS. Chemical control of charge transfer and recombination at semiconductor photoelectrode surfaces. *Inorg. Chem.*, 2005, 44, 6900–6911.
13. Kumar A, Wilisch WCA, Lewis NS. The electrical properties of semiconductor/metal, semiconductor/liquid, and semiconductor/conducting polymer contacts. *Crit. Rev. Solid State Mater. Sci.*, 1993, 18, 327–353.
14. Das S, Daud WMA. A review on advances in photocatalysts towards CO_2 conversion. *RSC Adv.*, 2014, 4, 20856–20893.
15. Inoue T, Fujishima A, Konishi S, Honda K. *Nature*, 1979, 277, 637–638.
16. Das S, Daud WMAW. Photocatalytic CO_2 transformation into fuel: A review on advances in photocatalyst and photoreactor. *Renew. Sust. Energy. Rev.*, 2014, 39(14), 765–805.
17. Magdesieva T, Yamamoto T, Tryk D, Fujishima A. Electrochemical reduction of CO_2 with transition metal phthalocyanine and porphyrin complexes supported on activated carbon fibers. *J. Electrochem. Soc.*, 2002, 149(6), D89–D95.
18. Tahir M, Amin NS. *Appl. Catal., B*, 2013, 142–143, 512–522.
19. Van Grieken R, Aguado J, López-Mu˜ noz M, Marug´ an J. *J. Photochem. Photobiol., A*, 2002, 148, 315–322.
20. Tan SS, Zou L, Hu E. *Catal. Today*, 2006, 115, 269–273.
21. Fotou GP, Pratsinis SE. *Chem. Eng. Commun.*, 1996, 151, 251–269.
22. Yui T, Kan A, Saitoh C, Koike K, Ibusuki T, Ishitani O. *ACS Appl. Mater. Interfaces*, 2011, 3, 2594–2600.
23. Kaneco S, Kurimoto H, Shimizu Y, Ohta K, Mizuno T, *Energy*, 1999, 24, 21–30.
24. Kaneco S, Kurimoto H, Ohta K, Mizuno T, Saji A. *J. Photochem. Photobiol., A*, 1997, 109, 59–63.
25. Dey G, Belapurkar A, Kishore K. *J. Photochem. Photobiol., A*, 2004, 163, 503–508.
26. Stock M, Dunn S. *Ferroelectrics*, 2011, 419, 9–13.
27. Zhang K, Guo L. *Catal. Sci. Technol.*, 2013, 3, 1672–1690.
28. Hong J, Zhang W, Ren J, Xu R. Photocatalytic reduction of CO_2: A brief review on product analysis and systematic methods. *Anal. Methods*, 2013, 5, 1086–1097.
29. Yuan L, Xu YJ. Photocatalytic conversion of CO_2 into value-added and renewable fuels. *Appl. Surf. Sci.*, 2015, 342, 154–167.
30. Liu YY, Huang BB, Dai Y, Zhang XY, Qin XY, Jiang MH, Whangbo MH. Selective ethanol formation from photocatalytic reduction of carbon dioxide in water with $BiVO_4$ photocatalyst. *Catal. Commun.*, 2009, 11, 210–213.
31. Qin S, Xin F, Liu Y, Yin X, Ma W. Photocatalytic reduction of CO_2 in methanol to methyl formate over CuO–TiO_2 composite catalysts. *J. Colloid Interface Sci.*, 2011, 356, 257–261.
32. Yang CC, Yu YH, van der Linden B, Wu JCS, Mul G. Artificial photosynthesis over crystalline TiO_2-based catalysts: Fact or fiction? *J. Am. Chem. Soc.*, 2010, 132, 8398–8406.
33. Liu BJ, Torimoto T, Matsumoto H, Yoneyama H. Effect of solvents on photocatalytic reduction of carbon dioxide using TiO_2 nanocrystal photocatalyst embedded in SiO_2 matrices. *J. Photochem. Photobiol., A*, 1997, 108, 187–192.
34. Teramura K, Iguchi S, Mizuno Y, Shishido T, Tanaka T. Photocatalytic conversion of CO_2 in water over layered double hydroxides. *Angew. Chem. Int. Ed.*, 2012, 51, 8008–8011.
35. Lizuka K, Wato T, Miseki Y, Saito K, Kudo A. Photocatalytic reduction of carbon dioxide over Ag cocatalyst-loaded $ALa_4Ti_4O_{15}$ (A = Ca, Sr, and Ba) using water as a reducing reagent. *J. Am. Chem. Soc.*, 2011, 133, 20863–20868.

36. Joo F, Laurenczy G, Karady P, Elek J, Nadasdi L, Roulet R. Homogeneous hydrogenation of aqueous hydrogen carbonate to formate under mild conditions with water soluble rhodium(I)-and ruthenium(II)-phosphine catalysts. *Appl. Organomet. Chem.*, 2000, 14, 857–859.
37. Ganesh I. Conversion of carbon dioxide into methanol—a potential liquid fuel: Fundamental challenges and opportunities (a review). *Renew. Sust. Energ. Rev.*, 2014, 31, 221–257.
38. Omae I. Aspects of carbon dioxide utilization. *Catal. Today*, 2006, 115(1–4), 33–52.
39. Herman RG, Klier K, Simmons GW, Finn BP, Bulko JB, Kobylinski TP. Catalytic synthesis of methanol from CO-H_2. I. Phase composition, electronic properties, and activities of the Cu/ZnO/M_2O_3 catalysts. *J. Catal.*, 1979, 56(3), 407–429.
40. Ganesh I, Sekhar PSC, Padmanabham G, Sundararajan G. Influence of Lidoping on structural characteristics and photocatalytic activity of ZnO nanopowder formed in a novel solution pyro-hydrolysis route. *Appl. Surf. Sci.*, 2012, 259, 524–537.
41. Hirano K, Inoue K, Yatsu T. Photocatalyzed reduction of CO_2 in aqueous TiO_2 suspension mixed with copper powder. *J. Photochem. Photobiol. A: Chem.*, 1992, 64(2), 255–258.
42. Hemminger JC, Carr R, Somorjai GA. Photoassisted reaction of gaseous water and carbon dioxide adsorbed on $SrTiO_2$ (111) crystal face to form methane. *Chem. Phys. Lett.*, 1978, 57(1), 100–104.
43. Yang YX, Evans J, Rodriguez JA, White MG, Liu P. Fundamental studies of methanol synthesis from CO_2 hydrogenation on Cu(111), Cu clusters, and Cu/ZnO(000(1)overbar). *Phys. Chem. Chem. Phys.*, 2010, 12(33), 9909–9917.
44. Ichikawa S, Doi R. Hydrogen production from H_2O and conversion of CO_2 to useful chemicals by room temperature photoelectrocatalysis. *Catal. Today*, 1996, 27, 271–277.
45. Sakka S, Kamiya K, Makita K, Yamamoto Y. Formation of sheets and coating films from alkoxide solutions. *J. Non-Crystal Solids*, 1984, 63(1 and 2), 223–235.
46. Hinogami R, Nakamura Y, Yae S, Nakato Y. An approach to ideal semiconductor electrodes for efficient photoelectrochemical reduction of CO_2 by modification with small metal particles. *J. Phys. Chem. B*, 1998, 102, 974–980.
47. Gerischer H. Electrochemical photo and solar cells principles and some experiments. *J. Electroanal. Chem. Interfacial Electrochem.*, 1975, 58(1), 263–274.
48. Aurian-Blajeni B, Halmann M, Manassen J. Electrochemical measurements on the photoelectrochemical reduction of aqueous carbon dioxide on p-gallium phosphide and p-gallium arsenide semiconductor electrodes. *Sol. Energy Mater.*, 1983, 8, 425–440.